Sub-micrometre spherical particles of TiO_2, ZrO_2 and PZT by nebulized spray pyrolysis of metal–organic precursors

P. Murugavel, M. Kalaiselvam, A. R. Raju and C. N. R. Rao*

Jawaharlal Nehru Centre for Advanced Scientific Research, Jakkur, Bangalore—560 064, India and Materials Research Centre, Indian Institute of Science, Bangalore—560 012, India

Nebulized spray pyrolysis of metal–organic precursors in methanol solution has been employed to prepare powders of TiO_2, ZrO_2 and $PbZr_{0.5}Ti_{0.5}O_3$(PZT). This process ensures complete decomposition of the precursors at relatively low temperatures. The particles have been examined by scanning and transmission electron microscopy as well as X-ray diffraction. As prepared, the particles are hollow agglomerates of diameter 0.1–1.6 μm, but after heating to higher temperatures the ultimate size of the particles comprising the agglomerates are considerably smaller (0.1 μm or less in diameter) and crystalline.

Spray pyrolysis has been widely used to prepare a variety of materials.[1–3] Thus, micrometre-sized particles of Al_2O_3 and $CaAl_2O_4$ were prepared by Roy *et al.*[4] Several other oxides have also been prepared by spray pyrolysis by employing several variants of the techniques for atomization of the precursor solution which include pneumatic, ultrasonic and electrostatic methods. The droplet size, size distribution and the rate of atomization differ with the method employed for atomization. Spray pyrolysis consists of various steps which are atomization, precipitation, drying, thermolysis and sintering in the given order. Ultrasonic nebulization is a spraying technique in which ultrasound is focused at the surface of the liquid to produce micrometre sized droplets. This is a simple low-cost alternative for the deposition of high quality thin films of novel complex oxides.[5–7] In this laboratory, we have used nebulized spray pyrolysis to prepare oriented epitaxial films of several complex metal oxides.[8,9] This method essentially uses metal–organic precursors just as in MOCVD. Ultrasonic nebulizers have been recently used to prepare oxide materials such as ZnO,[10] stabilized zirconia,[11] $BaTiO_3$[12] and mullite.[13] In all these preparations, aqueous solutions of the relevant metal compounds have been employed and the particle size of the final oxide powders is of the order of 1 μm or higher. The use of aqueous solutions necessarily requires that the transducer employed in ultrasonic nebulization is outside the container so that it does not come in direct contact with the solution. However, if one uses metal salts in non-aqueous solvents, it would be possible to keep the solution in contact with the transducer which would lower the power required for nebulization. Besides, the use of organometallic precursors in organic solvents may be better for preparing powders of complex oxides with greater compositional homogeneity. We have employed nebulized spray pyrolysis of organometallic precursors and prepared submicrometre, spherical particles of TiO_2, ZrO_2 and $PbZr_{0.5}Ti_{0.5}O_3$.

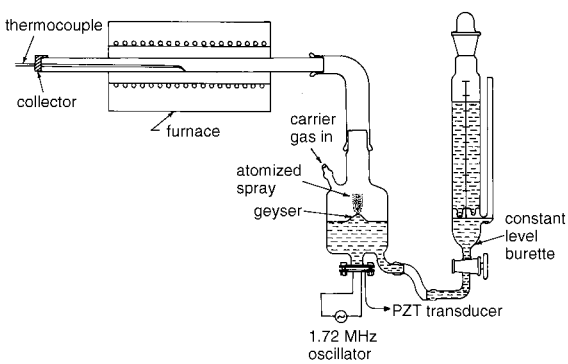

Fig. 1 Schematic diagram of the nebulized spray pyrolysis apparatus used for the preparation of spherical oxide particles

Experimental

We have employed titanium isopropoxide and zirconium isopropoxide precursors in methanol solution (0.1 M) for preparing TiO_2 and ZrO_2 powders respectively. In order to prepare

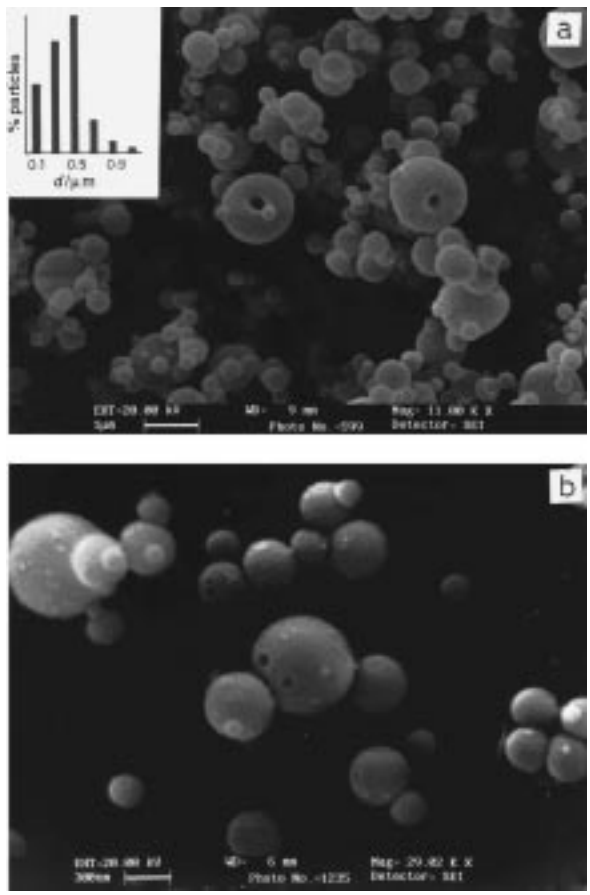

Fig. 2 Scanning electron micrographs of TiO_2 particles: (a) as obtained by nebulized spray pyrolysis at 723 K (the inset shows the particle size distribution of the powder) and (b) after heating the powder at 773 K for 12 h

powders of $PbZr_{0.5}Ti_{0.5}O_3$ (PZT), a methanol solution containing stoichiometric quantities of lead acetate, zirconium isopropoxide and titanium isopropoxide (0.05 M each) was employed. Dry air was used (5 l min^{-1}) as a carrier gas.

A schematic diagram showing different parts of the locally fabricated apparatus for ultrasonically nebulized spray pyrolysis is shown in Fig. 1. It consists of two zones: (*a*) the atomization chamber and (*b*) the pyrolysis reactor. The source liquid is kept in the atomization chamber and it is designed such that the bottom of the chamber has a cylindrical opening to fit the PZT transducer which oscillates at a frequency of 1.72 MHz. The special feature of this design is that the upper electrode of the PZT transducer is in direct contact with the source liquid. This gives the highest energy transfer to the liquid when compared to the non-contact method, which is used when there is a possibility of the electrode material

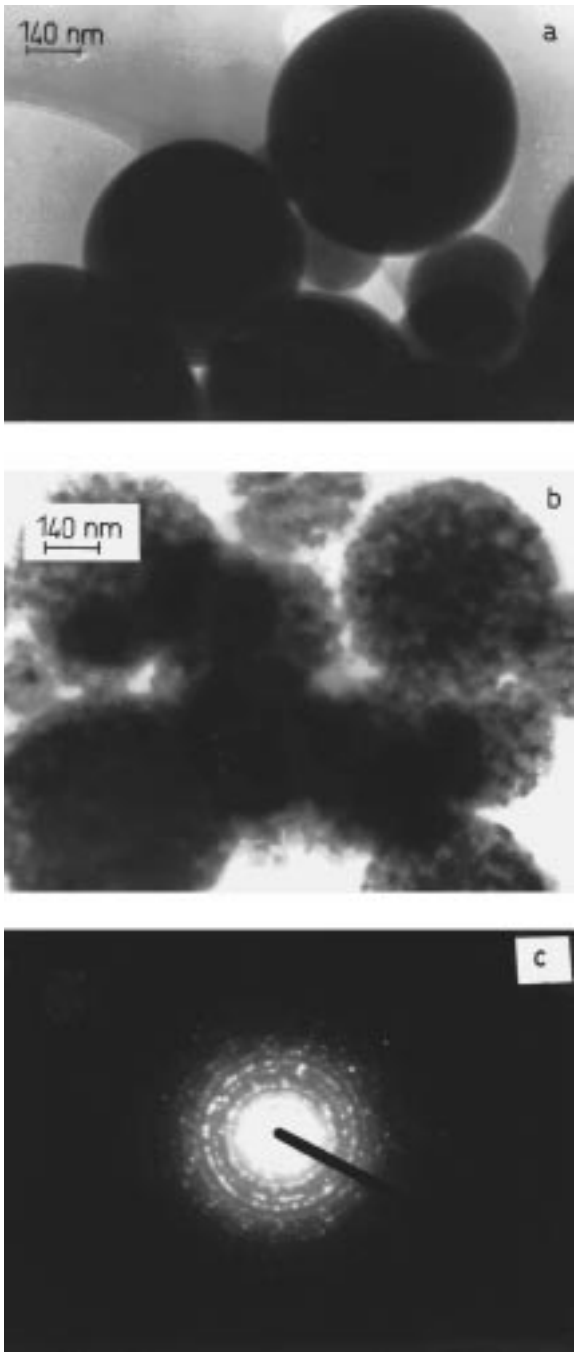

Fig. 3 Transmission electron micrographs of TiO_2 particles: (a) as obtained by nebulized spray pyrolysis at 723 K, (b) after heating the powder at 773 K for 12 h and (c) electron diffraction pattern of the powder heated at 773 K for 12 h

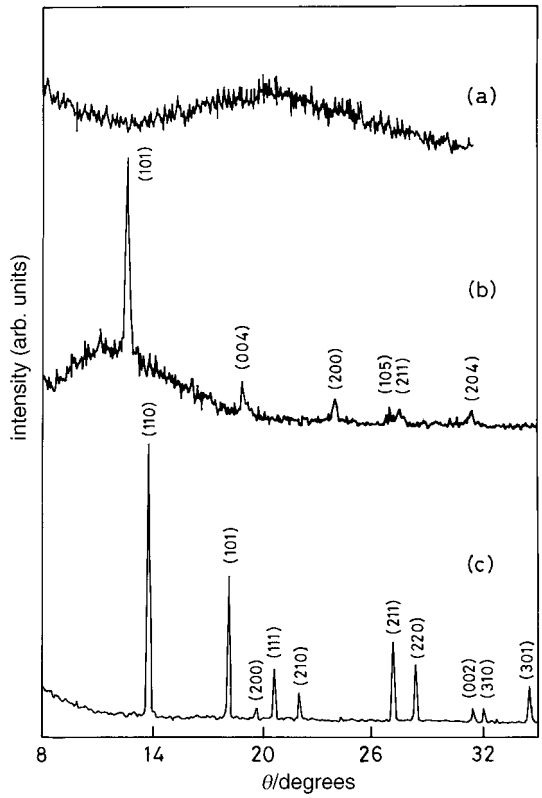

Fig. 4 X-Ray diffraction patterns of TiO_2 powders: (a) as obtained at 723 K, (b) after heating at 773 K for 12 h and (c) after heating at 1073 K for 12 h

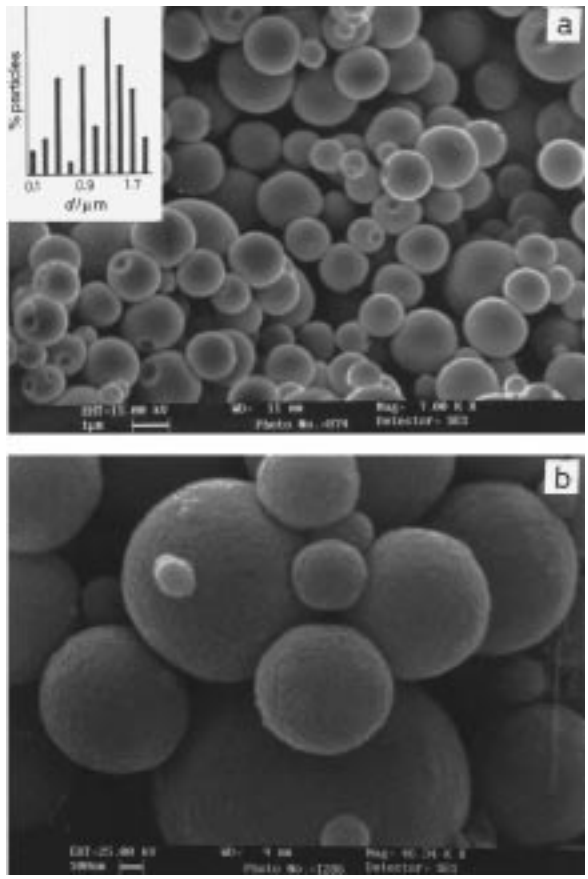

Fig. 5 Scanning electron micrographs of ZrO_2 particles: (a) as obtained by nebulized spray pyrolysis at 723 K (the inset shows the particle size distribution of the powder) and (b) after heating the powder at 773 K for 12 h

reacting with the solution. A minor disadvantage is that the liquid pH has to be maintained around 7. The liquid level in the atomization chamber is maintained by using a constant level burette which also allows the measurement of the volume of nebulized liquid.

When a high-frequency ultrasonic beam is directed at the liquid/gas interface through the PZT transducer a geyser forms at the surface of the liquid and the height of the geyser is proportional to the acoustic intensity and the physical properties of the liquid (vapour pressure, viscosity, density and surface tension). The geyser formation is accompanied by the cavitation at the liquid/gas interface. When the amplitude of the acoustic vibrations exceeds a certain threshold value, liquid atomization occurs. Above this threshold a continuous and regular mist (nebulized spray) is generated. The nebulized spray produced in the first chamber is transported by a carrier gas, which was dry air in all the experiments, introduced through a side-port. The second zone is a long quartz tube which is kept in a furnace at a preset temperature. The processes of drying and thermolysis take place in this zone and sintering is done in a separate furnace. The reason for having a single zone for drying and thermolysis is the following. If precipitation and drying occur slowly, there is a tendency for different components in the droplet to precipitate at different times which would lead to inhomogenity in the composition. The product consisting of fine powder is collected in a collector fixed at the other end of the quartz tube.

The morphology and particle size distribution were analyzed by employing a Leica S440i scanning electron microscope and a Quantimet Q500MC image analyser respectively and energy dispersive X-ray analysis was carried out by employing an Oxford instruments ISIS Si detector. Transmission electron microscope images were recorded with a JEOL 3010 microscope. The phase compositions of the powders obtained by the nebulized spray pyrolysis and subsequent heating at different temperature were determined by employing a Seifert 3000 X-ray powder diffractometer with Cu-Kα radiation (θ–θ geometry).

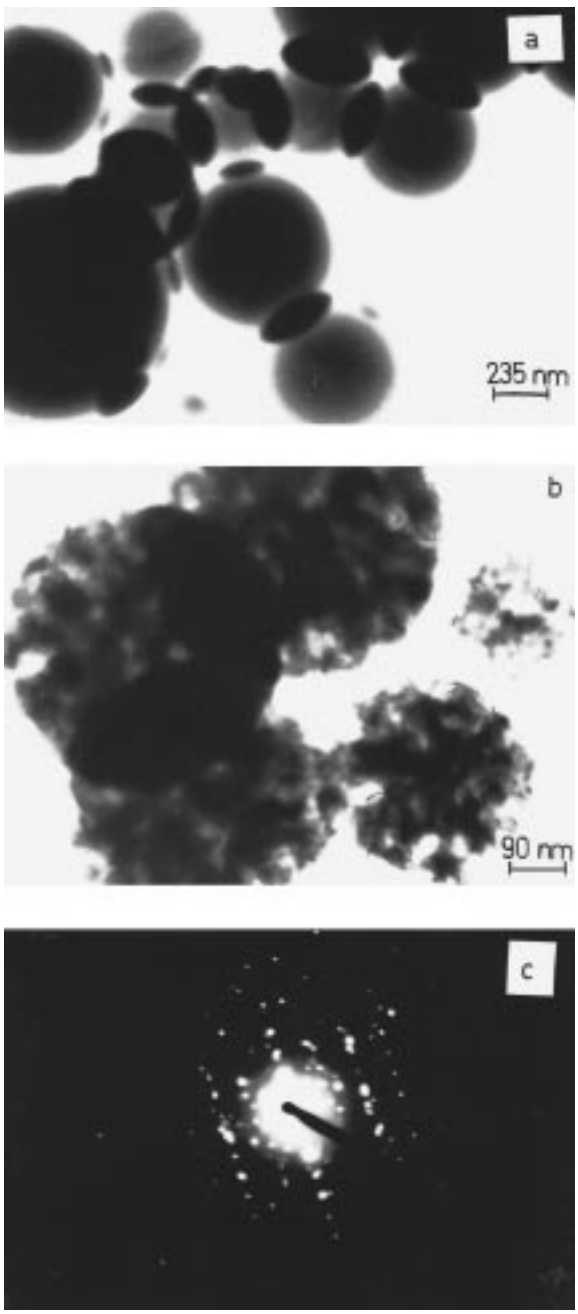

Fig. 6 Transmission electron micrographs of ZrO_2 particles: (a) as obtained by nebulized spray pyrolysis at 723 K, (b) after heating the powder at 773 K and (c) electron diffraction pattern of the powder heated at 1023 K for 12 h

Results and Discussion

TiO_2

Fig. 2(a) shows an SEM micrograph of the TiO_2 powder obtained after nebulized spray pyrolysis of a 0.1 M solution of

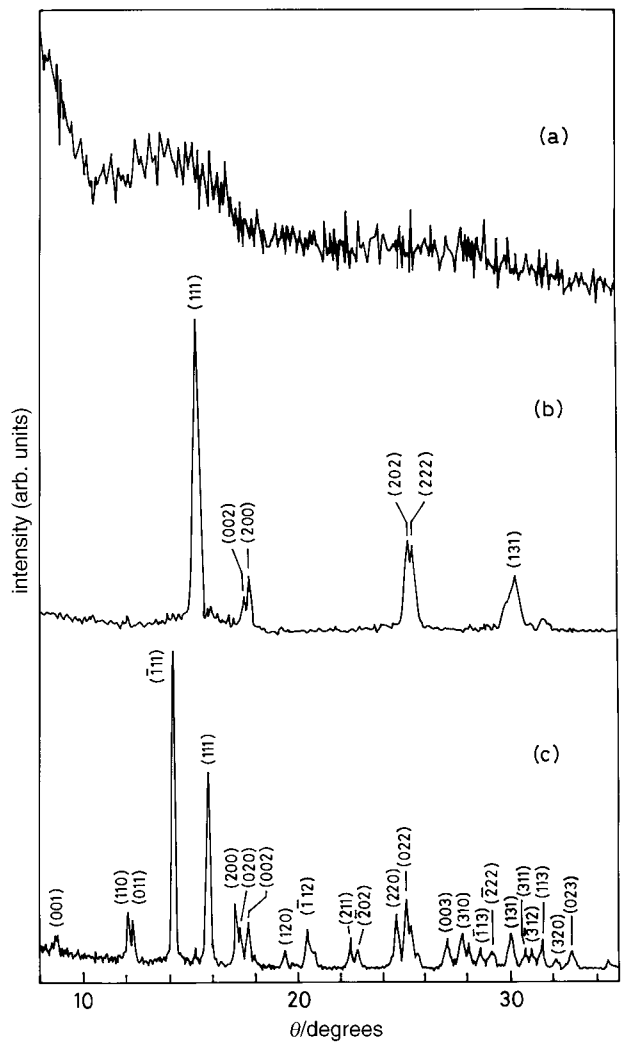

Fig. 7 X-Ray diffraction patterns of ZrO_2 powders: (a) as obtained at 723 K, (b) after heating at 773 K for 12 h and (c) after heating at 1073 K for 12 h

titanium isopropoxide in methanol at 723 K. The particles obtained are spherical or doughnut shaped. The particle size distribution shown in Fig. 2(a) suggests that most of the particles have a diameter in the range 0.3–0.5 μm. Some of the particles have cavities in them which are likely to result from predominant surface precipitation and fast evaporation of solvent. The particles are actually hollow spherical shells and shell fragments and the particle diameter of 0.3–0.5 μm truly corresponds to agglomerates of small individual particles of <0.1 μm diameter. A TEM image of the TiO_2 particles as obtained from nebulized spray pyrolysis is shown in Fig. 3(a). This image also confirms the spherical nature of the particles. Electron diffraction patterns show them to be amorphous and this is also confirmed by the X-ray diffraction pattern [Fig. 4(a)]. However, after heating the as-obtained particles at 773 K for 12 h they become crystalline. The X-ray diffraction pattern [Fig. 4(b)] shows the structure to correspond to that of anatase phase (JCPDS No. 21-1272) with $a=3.7986$ A and $c=9.5544$ A. The electron diffraction pattern shows spotty patterns [Fig. 3(c)] confirming the crystallization of TiO_2 particles on heating to 773 K. The SEM image of the anatase phase particles is shown in Fig. 2(b) and the corresponding TEM image in Fig. 3(b). These images establish that the particles remain spherical after crystallization. The TEM image also reveals how the large spherical particles are agglomerates and are actually composed of smaller particles (*ca.* 20 nm). We obtained the rutile phase of TiO_2 (JCPDS No. 22-1276) with $a=4.5949$ A and $c=2.9540$ A by heating the anatase powder at 1073 K for 12 h as indicated by the X-ray diffraction pattern in Fig. 4(c).

ZrO_2

Fig. 5(a) shows the SEM micrograph of the ZrO_2 powder obtained by the nebulized spray pyrolysis of the precursor solution at 723 K. The particles are spherical [Fig. 5(a)] and the size distribution of the particles indicates the diameter to be in the range 0.8–1.6 μm. The TEM micrograph in Fig. 6(a) also shows the spherical nature of these particles. The powder is amorphous as revealed by the electron and X-ray diffraction patterns and the latter is shown in Fig. 7(a). Heating the powder at 823 K for 12 h gives a tetragonal phase (JCPDS No. 17-923) with $a=5.0922$ A and $b=5.1958$ A [Fig. 7(b)]. SEM and TEM images of the powder heated to 823 K are shown in Fig. 5(b) and 6(b), respectively. The images show that the particles remain spherical after the heat treatment and that they are in turn composed of smaller particles (*ca.* 20 nm). Heating the tetragonal powder phase at 1023 K for 12 h resulted in the monoclinic phase (JCPDS No. 36-420) $a=5.3165$ A, $b=5.1867$ A, $c=5.1445$ A and $\beta=99.151°$, as confirmed by the X-ray diffraction pattern shown in Fig. 7(c).

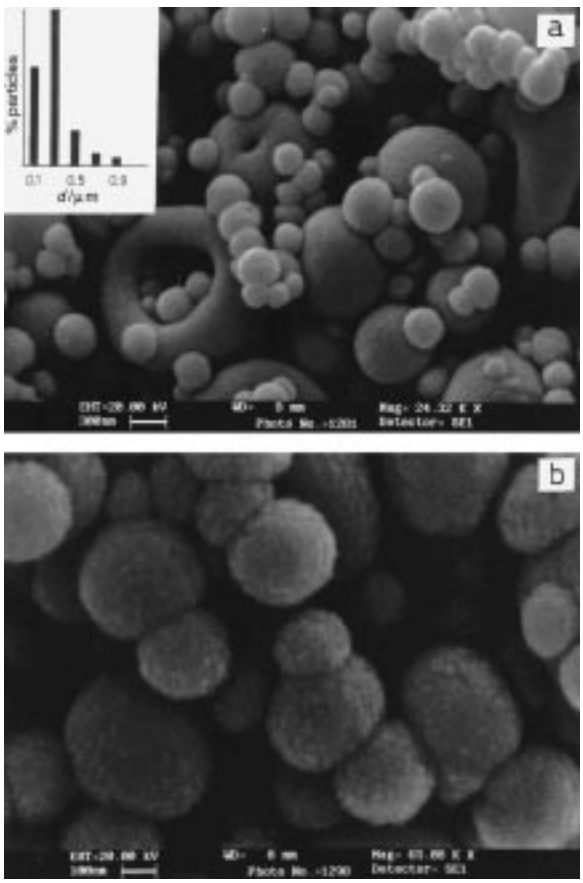

Fig. 8 Scanning electron micrographs of PZT particles: (a) as obtained by nebulized spray pyrolysis at 673 K (the inset shows the particle size distribution of the powder) and (b) after heating the powder at 823 K for 12 h

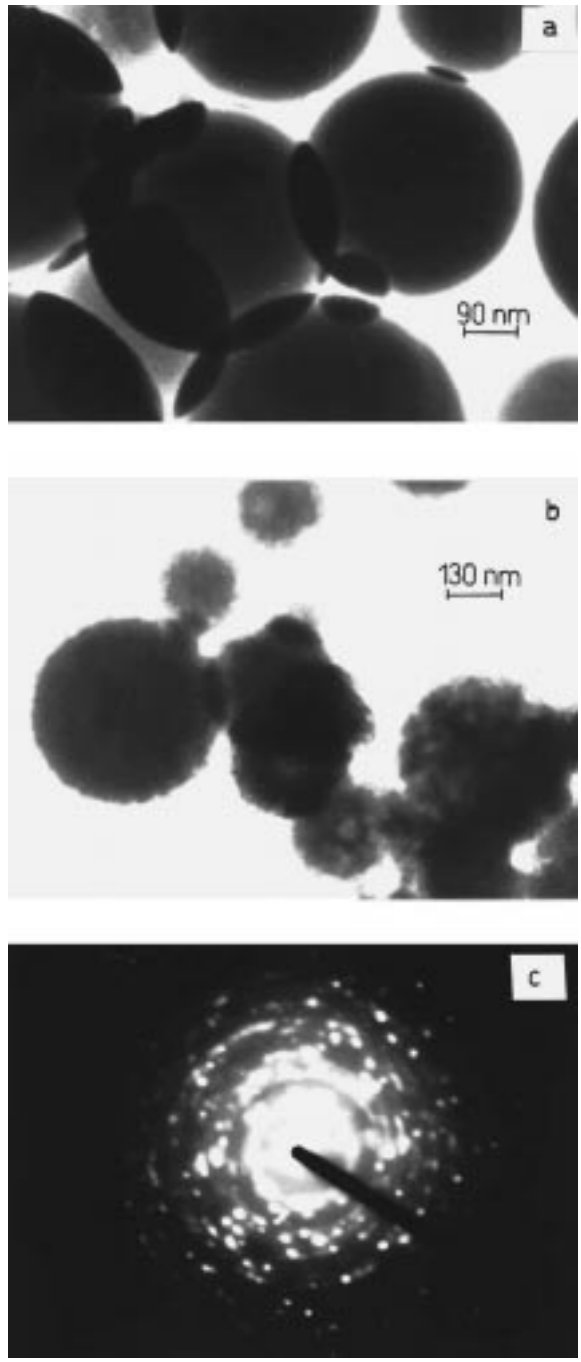

Fig. 9 Transmission electron micrographs of PZT particles: (a) as obtained by nebulized spray pyrolysis at 673 K, (b) after heating the powder at 823 K and (c) electron diffraction pattern of the powder after heating at 823 K for 12 h

PZT

The SEM and TEM images of the powders of PZT as obtained by nebulized spray pyrolysis of the precursor solution at 673 K are shown in Fig. 8(a) and 9(a), respectively. The particle size distribution shown as an inset in Fig. 8(a) suggest the diameter to be in the range 0.1–0.5 μm. This powder is amorphous as revealed by the electron and X-ray diffraction patterns and the latter is shown in Fig. 10(a). After heating the amorphous powder at 823 K for 12 h, it transformed into the stable tetragonal phase (JCPDS No. 33-784) with $a=4.0655$ A and $c=4.0646$ A. The X-ray diffraction pattern of the powder heated to 823 K is shown in Fig. 10(b). The SEM and TEM micrographs of these particles in Fig. 8(b) and 9(b) show them to be spherical even after crystallization. The large spherical particles are composed of smaller particles (20–30 nm) just as in the case of TiO_2 and ZrO_2. Energy dispersive X-ray analysis (Fig. 11) of the PZT powder was analyzed for quantitative elemental composition by employing the SEMQuant software with ZAF correction procedure. This gave a Pb:Zr:Ti ratio of 1:0.5:0.5, confirming the composition to be $PbZr_{0.5}Ti_{0.5}O_3$.

Fig. 12(a) shows a TEM image to illustrate how the particles

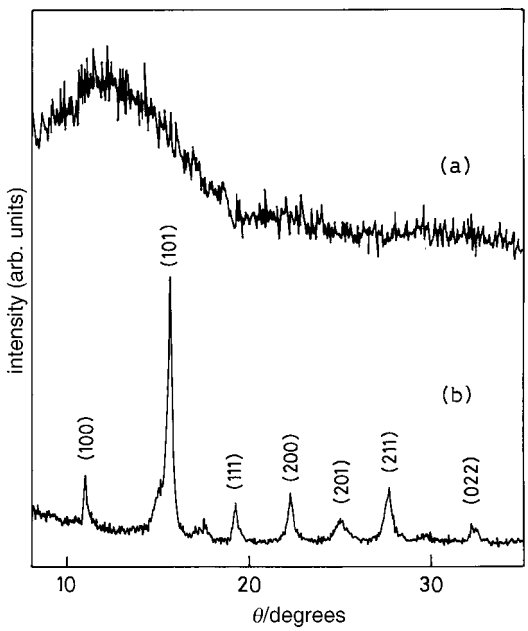

Fig. 10 X-Ray diffraction patterns of PZT powder: (a) as obtained at 723 K, (b) after heating at 823 K for 12 h

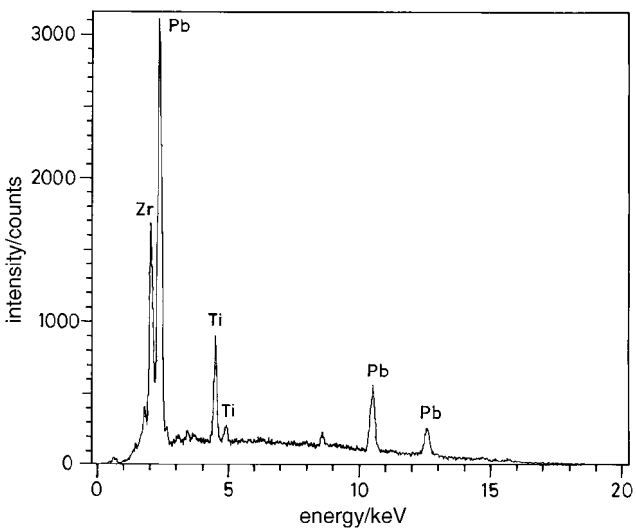

Fig. 11 EDAX spectrum of the $PbZr_{0.5}Ti_{0.5}O_3$ powder

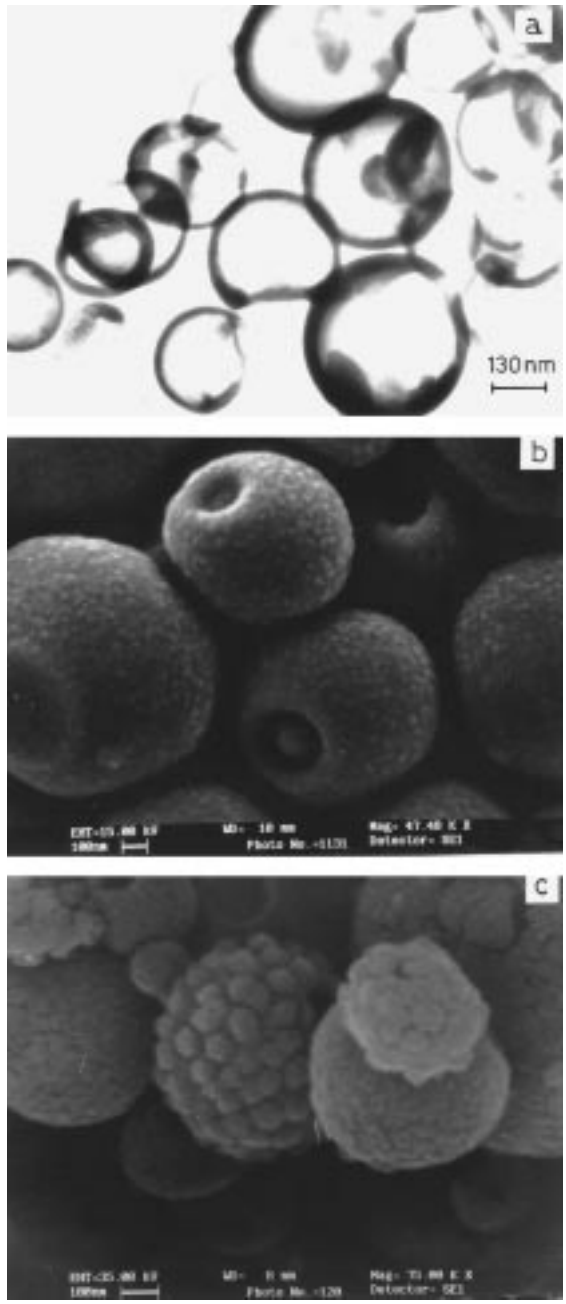

Fig. 12 (a) TEM of PZT spheres and shells as obtained from nebulized spray pyrolysis, (b) high magnification SEM image of ZrO_2 heated to 773 K, (c) high magnification SEM image of PZT heated to 823 K

are hollow. These hollow spherical particles obtained by pyrolysis are generally composed of smaller particles as mentioned earlier. This is clearly seen from Fig. 12(b) and (c) where high magnification SEM images of the crystalline particles of ZrO_2 and PZT are shown. It thus appears that although the particle size distributions in Fig. 2(a), 5(a) and 8(a) give diameters up to 1 μm or more, the ultimate size of the particles is much smaller. Thus, the size of the larger agglomerated spherical particles of ZrO_2 in Fig. 12(b) and of PZT in Fig. 12(c) are in the range 0.5–1.5 μm, but the small particles comprising these are fairly uniform with mean diameters of <0.1 μm.

Conclusion

The present study of the preparation of metal oxide powders by nebulized spray pyrolysis of metal–organic precursors establishes the efficacy of the method. It has certain noteworthy features as detailed overleaf.

(*i*) The use of metal–organic precursors ensures complete decomposition at relatively low temperatures.

(*ii*) The particles as-obtained from nebulized spray pyrolysis are spherical and have diameters in the range 0.1–1.6 μm.

(*iii*) Some of the particles are collapsed shells or hemispheres. Most are however hollow and are composed of considerably smaller particles of 0.1 μm diameter or less.

References

1 D. W. Sproson and G. L. Messing, in *Ceramic Powder Science*, ed. G. L. Messing, K. S. Mazdiyasni, J. W. McCauley and R. A. Haber, American Ceramic Society, Westerville, OH, 1987.
2 G. L. Messing, S. C. Zhang and G. V. Jayanthi, *J. Am. Ceram. Soc.*, 1993, **76**, 2707.
3 R. Stevens, *Trans. J. Br. Ceram. Soc.*, 1981, **80**, 81.
4 D. M. Roy, R. R. Neurgaonkar, T. P. O'Holleran and R. Roy, *Am. Ceram. Soc. Bull.*, 1981, **56**, 1023.
5 W. W. Xu, R. Kershaw, K. Dwight and A. Wold, *Mater. Res. Bull.*, 1990, **25**, 1385.
6 M. Langlet and J. C. Joubert, in *Chemistry of Advanced Materials*, ed. C. N. R. Rao, IUPAC, 21st Century Monogr. Ser., Blackwell, Oxford, 1993.
7 A. R. Raju, H. N. Aiyer and C. N. R. Rao, *Chem. Mater.*, 1995, **7**, 225.
8 A. R. Raju, H. N. Aiyer and C. N. R. Rao, in *Interfacial Science*, ed. M. W. Roberts, IUPAC, 21st Century Monogr. Ser., Blackwell, Oxford, 1997.
9 H. N. Aiyer, A. R. Raju and C. N. R. Rao, *Chem. Mater.*, 1997, **9**, 755.
10 T. Q. Liu, O. Sakurai, N. Mizutani and M. Kato, *J. Mater. Sci.*, 1986, **21**, 3698.
11 B. Dubois, D. Ruffier and P. Odier, *J. Am. Ceram. Soc.*, 1989, **72**, 713.
12 O. Milosevic and D. Uskokovic, *Mater. Sci. Eng. A*, 1993, **168**, 249.
13 Dj. Janackovic, V. Jokanovic, Lj. Kostic-Gvozdenovic, Lj. Zivkovic and D. Uskokovic, *J. Mater. Res.*, 1996, **11**, 1706.

Paper 7/00301C; *Received* 13*th January*, 1997